Building Complex Hybrid Carbon Architectures by Covalent Interconnections: Graphene–Nanotube Hybrids and More

Ruitao Lv,[†] Eduardo Cruz-Silva,[‡] and Mauricio Terrones[‡,§,⊥,*]

[†]Key Laboratory of Advanced Materials (MOE), School of Materials Science and Engineering, Tsinghua University, Beijing 100084, China, [‡]Department of Physics and Center for 2-Dimensional and Layered Materials, The Pennsylvania State University, University Park, Pennsylvania 16802, United States, [§]Department of Chemistry and Department of Materials Science & Engineering, The Pennsylvania State University, University Park, Pennsylvania 16802, United States, and [⊥]Faculty of Engineering, Shinshu University, Wakasato 4-17-1, Nagano 380-8553, Japan

ABSTRACT Graphene is theoretically a robust two-dimensional (2D) sp^2-hybridized carbon material with high electrical conductivity and optical transparency. However, due to the existence of grain boundaries and defects, experimentally synthesized large-area polycrystalline graphene sheets are easily broken and can exhibit high sheet resistances; thus, they are not suitable as flexible transparent conductors. As described in this issue of *ACS Nano*, Tour *et al.* circumvented this problem by proposing and synthesizing a novel hybrid structure that they have named "rebar graphene", which is composed of *covalently* interconnected carbon nanotubes (CNTs) with graphene sheets. In this particular configuration, CNTs act as "reinforcing bars" that not only improve the mechanical strength of polycrystalline graphene sheets but also bridge different crystalline domains so as to enhance the electrical conductivity. This report seems to be only the tip of the iceberg since it is also possible to construct novel and unprecedented hybrid carbon architectures by establishing *covalent* interconnections between CNTs with graphene, thus yielding graphene–CNT hybrids, three-dimensional (3D) covalent CNT networks, 3D graphene networks, *etc.* In this Perspective, we review the progress of these carbon hybrid systems and describe the challenges that need to be overcome in the near future.

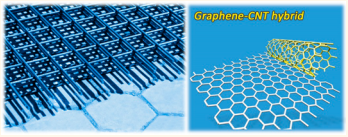

Carbon has always been a fascinating element to chemists, physicists, materials scientists, biologists, and engineers. It is not only crucial for constructing building blocks in living organisms, but it can also serve as a building unit in different carbon nanostructures exhibiting unprecedented physical and chemical properties. It is noteworthy that carbon is so far the only element that can form zero-dimensional (0D), one-dimensional (1D), two-dimensional (2D), and three-dimensional (3D) elemental crystal nanostructures (Figure 1). In particular, sp^2-hybridized carbon nanostructures have been successfully synthesized over the past decades, such as the 0D fullerenes,[1] 1D carbon nanotubes (CNTs),[2,3] 1D graphene nanoribbons (GNRs),[4] and 2D graphene sheets.[5] Furthermore, if CNTs (1D) and/or graphene (2D) can be covalently merged, novel 2D or 3D sp^2-hybridized carbon structures could be obtained. The electronic, mechanical, and surface properties of these hybrid systems would be significantly different. It is expected that these novel systems would display unique physicochemical properties and could then be used for construction of next-generation electronic and energy conversion/storage devices, electron field emission sources, thermal dissipation coatings, oil adsorption materials, *etc.* In this Perspective, we highlight important aspects related to the theoretical prediction, experimental synthesis, and physicochemical properties of different hybrid carbon systems that are based on establishing covalent interconnections among different sp^2-hybridized carbon structures, including graphene–CNT hybrids, 3D covalent CNT networks, 3D graphene networks, *etc.* We also highlight the Tour group's recent pioneering work on "rebar graphene" (a graphene–CNT hybrid),[6] which appears in this issue of *ACS Nano*, as well as describe the challenges in the synthesis and multifunctional properties of sp^2-hybridized carbon hybrid nanostructures.

Graphene and Hybrid Materials of Carbon. Graphene, an atomically thin layer of carbon, possesses unique properties due to its 2D morphology and displays outstanding properties such as high room-temperature

* Address correspondence to mut11@psu.edu.

Published online May 27, 2014
10.1021/nn502426c

© 2014 American Chemical Society

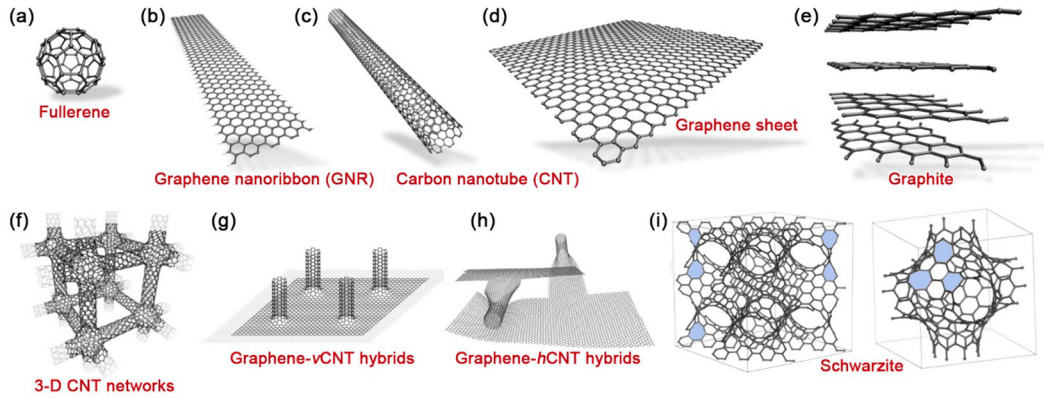

Figure 1. Dimensionality of sp^2-hybridized carbon nanostructures. (a) Fullerene (0D); (b) graphene nanoribbon (GNR) (1D); (c) carbon nanotube (CNT) (1D); (d) graphene sheet (2D); (e) graphite (3D); (f) 3D CNT networks (3-D); (g) hybrid of graphene with vertical CNT (*v*CNT) (3D); (h) hybrid of graphene with horizontal CNT (*h*CNT) (3D); and (i) graphene triple periodical minimal surfaces (or Schwarzites 3D graphene) showing nonhexagonal rings (*e.g.*, heptagons) highlighted.

carrier mobility,[7] high thermal conductivity,[8] room-temperature quantum Hall effect,[9] *etc*. It should be emphasized that the above-mentioned properties of monolayer graphene strongly depend on the degree of crystallinity, edge morphology, defect content, *etc*. Furthermore, its properties can significantly vary by simply stacking other graphene layer(s) on top. There are two main routes used for the synthesis of graphene: "top-down" (*e.g.*, mechanical exfoliation,[5] chemical exfoliation[10]) and "bottom-up" (*e.g.*, chemical vapor deposition (CVD),[11,12] synthetic polymerization of aromatic molecules[13]). In particular, the reduction of graphene oxide (rGO)[10,14] and CVD[11,12] are two commonly used methods for graphene synthesis. However, in the rGO route, as-synthesized graphene layers tend to aggregate (stack together) to form layered structures in a dry state. For CVD-derived monolayer graphene, the products are usually *polycrystalline*, which significantly diminishes their electronic and mechanical strength (theoretically predicted Young's moduli to be ~1 TPa)[15] due to the existence of large amounts of grain boundaries (heptagon−pentagon defect lines) and other types of vacancy-like defects. In addition, metal substrates (*e.g.*, Cu foil,[12] Ni film[11]) are usually used to produce highly crystalline graphene by CVD. Unfortunately, when large-area monolayer graphene sheets are detached from these metal substrates (*e.g.*, Cu foils), they can easily tear and break during wet transfer, if done without depositing a top protective polymer layer (*e.g.*, poly(methyl methacrylate) (PMMA), polydimethylsiloxane (PDMS)).[12] Therefore, it is important to synthesize novel hybrid sp^2-hybridized carbon structures that are able to inhibit the stacking of layers and to increase the in-plane mechanical strength in order to obtain polymer-free and robust graphene-like monolayers.

Additionally, if CNTs can be vertically intercalated between adjacent rGO layers, the aggregation (or stacking) of graphene layers will effectively be avoided. Recent theoretical work has predicted that the electronic transport,[16] thermal transport,[17] and hydrogen storage[18] properties would be remarkably enhanced by constructing covalently interconnected CNT−graphene hybrid nanostructures (see Figure 1g). However, if CNTs could be horizontally and covalently interconnected with large-area graphene sheets (see Figure 1h), their mechanical strength would also be significantly reinforced in virtue of the excellent flexibility and strength of CNTs. In this way, CNTs would promote fast charge transport pathways in polycrystalline graphene sheets, thus decreasing their sheet resistance. However, studies of planar single-walled CNT/graphene hybrids are still very scarce, except for the recent breakthroughs achieved by the Jiang group on "vein-membrane-like" hybrid films[19] and by the Tour group on "rebar graphene",[6] whose findings are published in the issue of *ACS Nano*. In addition to the graphene−CNT hybrid systems mentioned above, it is possible to construct two other possible 3D hybrids using graphene and CNTs as building blocks: 3D covalent CNT networks and 3D graphene covalent networks (see Figure 1). Below, we review the progress along these lines of research.

> In this issue of *ACS Nano*, the Tour group has proposed an alternative and effective strategy for obtaining transparent and highly conducting graphene−CNT hybrid films, which they term "rebar graphene".

Graphene−CNT Hybrids. Graphene−CNT hybrid nanostructures can be classified into two main categories: *CNT-rich* hybrids and *graphene-rich* hybrids (see Figure 2). In the former, small graphene layers/sheets could be anchored/attached on the *outer walls*[20] or *inner cores*[21] of CNTs. In this

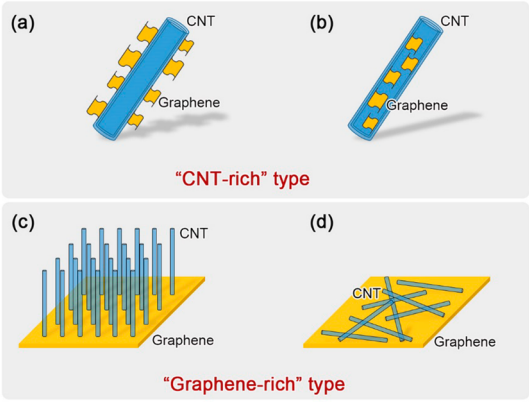

Figure 2. Different configurations of graphene–carbon nanotube hybrid nanostructures. Based on the *matrix* material, they can be roughly classified into two categories: "CNT-rich" type and "graphene-rich" type. (a) Graphene sheets unzipped from the *outer* walls of CNTs. Examples can be found in ref 20. (b) Graphene sheets derived from the *inner* walls of CNTs (see ref 21). (c) CNTs stand *vertically* on graphene sheets to form pillared arrays (examples can be found in refs 22–24). (d) CNTs spread *horizontally* on graphene sheets (examples can be found in refs 6, 19, and 25).

context and under harsh oxidation conditions, the outer walls of few-walled CNTs (*e.g.*, double-walled and triple-walled CNTs) could be partially unzipped, thus creating loose graphene sheets protruding out from CNTs. This type of CNT–graphene hybrid could serve as an excellent oxygen reduction electrocatalyst.[20] In this particular configuration, the graphene fragments created after the unzipping process increase the presence of more catalytic sites, while the inner walls of the CNTs facilitate fast charge transport during electrocatalysis due to their high electrical conductivity (Figure 2a). Another possible configuration for the "CNT-rich" hybrid is illustrated in Figure 2b. For example, by maintaining a weak oxidation atmosphere (*e.g.*, trace amount of H_2O vapor) during CNT growth, fragments of graphene layers get unzipped from the inner cores of the CNT, thus creating extra sites for immobilizing well-dispersed noble metal catalyst nanoparticles (*e.g.*, PtRu). Our previous work has demonstrated that as-synthesized CNT–graphene hybrids can be used as high-performance catalytic supports for the methanol electro-oxidation (MEO) reaction.[21]

Another group of graphene–CNT hybrids is the *graphene-rich* type, which is illustrated in Figure 2c,d. As mentioned above, large graphene flakes derived from rGO tend to aggregate together into layered stacked architectures, thus losing the integrity of the monolayers. However, if CNTs can stand *vertically* between two adjacent graphene layers, the aggregation will be effectively hampered and the porosity of the hybrid materials will increase (Figure 2c). For example, the Brunauer–Emmett–Teller (BET) surface area of graphene can be improved three times (from 202 to 612 m^2/g) after the intercalation of vertically aligned CNTs between the graphene layers.[23] When this kind of graphene–CNT hybrid is synthesized, metal catalysts (*e.g.*, Co,[23] Fe[24,26]) are necessary for the growth of vertical CNT pillars. The graphene can be obtained either from the rGO route[23,26] or from CVD growth.[24] Interestingly, as-synthesized graphene–CNT hybrids have demonstrated outstanding electrochemical properties and high cycle stability in supercapacitor applications.[23,24] Another configuration for *graphene-rich* hybrids is shown in Figure 2d, which corresponds to CNTs spreading/interconnecting *horizontally* within graphene sheets. In this context, the Terrones group proposed a self-assembly method for preparing hybrid paper-like films (Figure 3a–c) composed of alternating layers of rGO and different types of multi-walled carbon nanotubes (MWNTs) (Figure 3d–f).[25] As-obtained rGO–MWNT hybrid films show high mechanical robustness (Figure 3b,c) and excellent field emission properties when operating at very low voltage (*ca.* 0.55 V/μm).[25] However, due to the presence of stacked structures of many alternating graphene and MWNT layers, these hybrid paper-like films are relatively thick and are not transparent (similar to Xerographic paper).

If we intend to obtain an optically transparent and large-area graphene–CNT hybrid film for flexible transparent conducting electrode applications, CVD-derived graphene might be a better choice than self-assembled rGO sheets. Figure 4 demonstrates two strategies for achieving graphene–CNT hybrid *thin films* interconnected with CNT networks. As is well-known, CNT yarns and films can be directly drawn from highly oriented (or superaligned) CNT arrays.[27–30] Based on this technique, large-area MWNT thin films can be used to cover CVD-derived graphene sheets to form a graphene–CNT hybrid structure, as illustrated in Figure 4a. As-prepared *vein-membrane-like* hybrid films possess good electrical conductivity, optical transparency, and excellent mechanical strength. These materials could thus serve as ideal transmission electron microscopy (TEM) sample supports and gate electrodes for vacuum-operated electronics.[19] However, as shown in Figure 4b, the optical transmittance is not high (*e.g.*, 52.5% at 600 nm[19]) due to the relatively thick MWNT films. In addition, the interconnections between CNTs and graphene might be occurring *via* van der Waals' interactions or π–π stacking rather than covalent bonding. Fortunately, in this issue of *ACS Nano*, the Tour group has proposed an alternative, effective strategy for obtaining transparent and highly conducting graphene–CNT hybrid films, which they term "rebar graphene" (Figure 4c). The authors functionalized single-walled CNTs

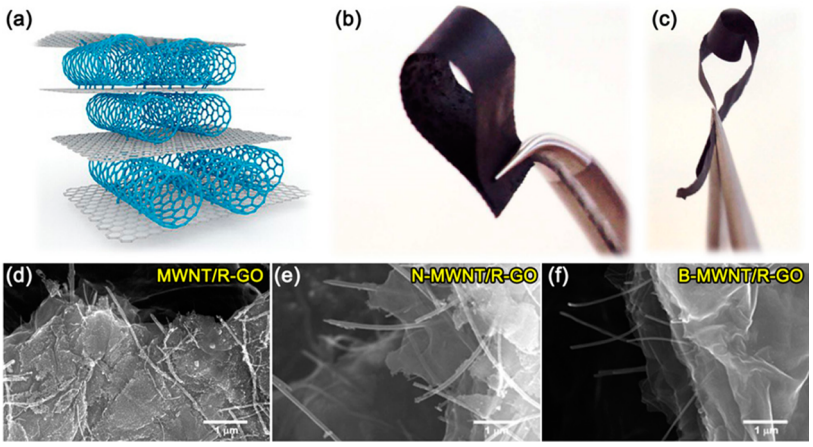

Figure 3. Hybrid paper-like films of alternating graphene and multiwalled carbon nanotube (MWNT) layers. (a) Schematic model of the graphene–MWNT hybrid film. (b,c) Photographs of hybrid paper made of MWNTs and graphene oxide (GO) before reduction. Typical scanning electron microscopy (SEM) images of (d) MWNT, (e) nitrogen-doped MWNTs (N-MWNTs), and (f) boron-doped MWNTs (B-MWNTs) with reduced GO (rGO) layers. Adapted from ref 25. Copyright 2013 American Chemical Society.

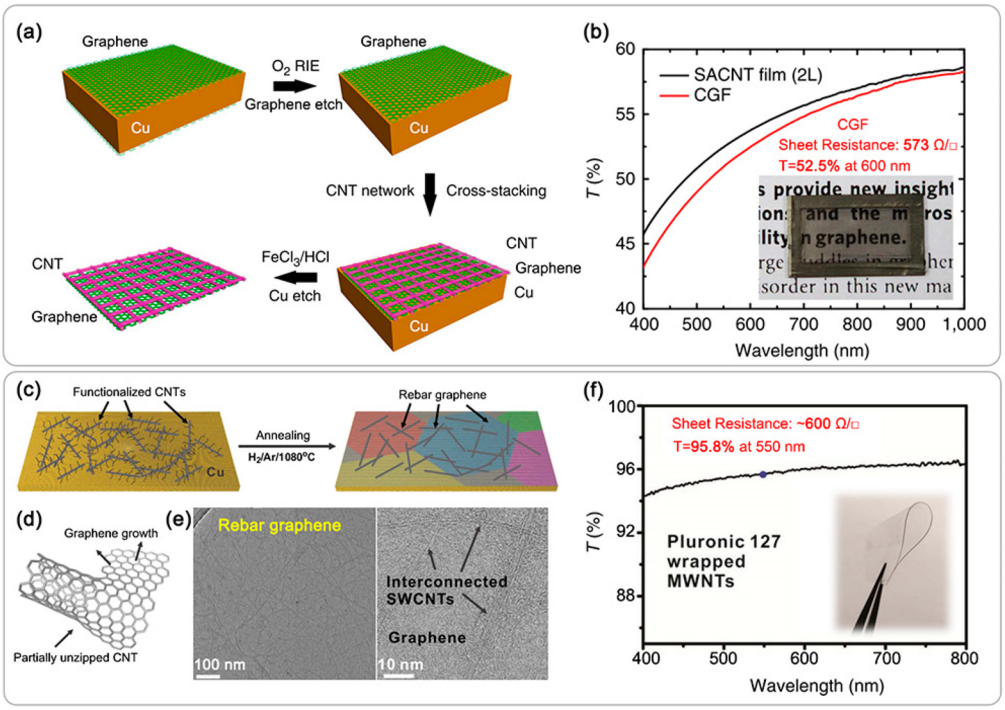

Figure 4. Graphene–carbon nanotube hybrid nanostructures with CNTs distributing horizontally on chemical vapor deposition (CVD)-derived graphene sheets. (a) Scheme for the fabrication of CNT/graphene hybrid film (CGF). Here, "RIE" denotes oxygen reactive-ion etching. (b) Optical transmittance of the CGF and superaligned CNT (SACNT) film. Here, "T" denotes optical transmittance (%). The inset shows the photograph of a CGF suspended on a stainless steel frame. Adapted with permission from ref 19. Copyright 2013 Nature Publishing Group. (c) Scheme for the synthesis of rebar graphene sheets, which was achieved on Cu foils by heating functionalized CNTs at 1080 °C for 15 min. (d) Scheme for graphene growth from the edges of a partially unzipped single-walled CNT (SWCNT). (e) Transmission electron microscopy (TEM) images indicating the formation of interconnected SWCNT networks in rebar graphene. (f) UV–vis spectrum and sheet resistance of rebar graphene sheets derived from Pluronic 127 wrapped multiwalled nanotubes. The inset is the corresponding photograph of a bent rebar graphene sheet transferred onto a polyethylene terephthalate (PET) substrate. Adapted from ref 6. Copyright 2014 American Chemical Society.

(*e.g.*, dodecyl-functionalized single-wall CNTs, Pluronic 127 wrapped MWNTs), which were then deposited on Cu foils and loaded into a CVD reaction chamber at ~1 mTorr. The reactor temperature was increased to 1080 °C, and then 500 sccm H_2 was introduced into the chamber for 10 min. Subsequently, CNT-coated Cu foil was quickly moved into the hot region and annealed for 90 s. After that, 0.7 sccm CH_4 as an extra carbon source for large-area graphene growth was introduced into the CVD chamber

for 15 min. Finally, the CH_4 flow was cut off, and the Cu foil was quickly removed from the hot region and cooled to room temperature. Isolated rebar graphene films were then obtained after etching away the Cu foil. In this hybrid nanostructure, CNTs act as a reinforced bar (or "rebar") for improving the mechanical strength and electrical conductivity of the graphene sheets. By using bright-field scanning transmission electron microscopy (BF-STEM), the authors further confirmed the presence of covalent interconnections between CNTs and graphene—some parts of the graphene are derived from partially unzipped CNTs (Figure 4d). Moreover, CNTs can form a network and thus serve as conducting pathways across grain boundaries of polycrystalline graphene sheets (Figure 4e). Meanwhile, the high optical transparency of graphene sheets is preserved because the CNTs are sparsely distributed on the graphene. Figure 4f depicts a UV−vis spectrum of a rebar graphene sheet grown from functionalized MWNTs. Interestingly, low sheet resistance (~600 Ω/□) and high transmittance (95.8% at 550 nm) were observed. Furthermore, as-obtained rebar graphene shows good mechanical flexibility. When it is transferred onto a polyethylene terephthalate (PET) substrate, rebar graphene can be bent freely, which is ideal for constructing flexible and transparent conducting films (inset of Figure 4f).[6]

Rebar graphene now represents a new group of sp^2-hybridized carbon nanostructures, and further studies on this material will certainly follow. For example, due to its high optical transmittance and low sheet resistance, rebar graphene can be readily used as flexible all-carbon transparent conducting electrodes, as demonstrated by the Tour group.[6] In addition, it may also find applications as a flexible carrier transport layer useful in organic photovoltaics.[31] Furthermore, if rebar graphene can be doped with other heteroatoms (*e.g.*, nitrogen doping), these doped materials might be used as a novel metal-free electrocatalyst for oxygen reduction reactions.[20] Due to the high mechanical strength of the hybrid film, rebar graphene could also be used as a robust and high-efficiency osmosis membrane in seawater desalination.[32]

Rebar graphene now represents a new group of sp^2-hybridized carbon nanostructures, and further studies on this material will certainly follow.

3D Covalent CNT Networks. As mentioned above, if we only use CNTs as building blocks, it is possible to construct 3D CNT networks.[33] This idea has attracted a great deal of attention following the successful synthesis of single-walled CNTs (SWCNTs).[34−36] From an electronics standpoint, serial or parallel circuits composed of CNTs can be important in the fabrication of future carbon-based electronic devices. However, in order to construct such circuits, a major challenge will be determining how to assemble CNTs covalently, preserving their excellent electronic, thermal, and mechanical properties.[37] In this context, highly crystalline CNTs possess an almost inert surface, and covalent bonds among tubes would need to be established *via* defects after some physical or chemical treatments. Methods for the synthesis of CNT junctions and networks include template-assisted routes,[38−40] electron beam irradiation processes,[41,42] the use of atomic welders that are able to interconnect CNTs (*e.g.*, boron,[43] sulfur[44]), secondary CVD growth using metal deposited on CNTs,[45,46] *etc.* Typical photographs and microstructures of 3D covalently interconnected B-doped CNTs can be seen in Figure 5a−d. More interestingly, 3D covalently bonded CNT networks seem to be highly relevant in electronics (*e.g.*, transparent electrodes,[47] thin-film transistors,[48] sensors[49]), bioapplication devices (*e.g.*, artificial muscles,[50] cell growth scaffolds[51]), strain gauge,[52] oil absorption applications,[43] *etc.* However, there are still many more investigations that need to be carried out along these lines. For example, how can one obtain periodic CNT networks in controllable ways? In addition, most published work on 3D networks deals with MWNTs instead of few-walled CNTs, and the synthesis of SWCNT networks remains an experimental challenge. Furthermore, alternative novel applications of 3D CNT networks are also waiting to be explored, such as bone tissue regeneration, catalyst supports, *etc.*

3D Graphene Networks. Integrating individual 2D graphene sheets into macroscopic 3D networks is also crucial for facilitating their possible applications in diverse areas. To achieve this goal, there are two strategies that can be adopted. One is to construct graphene-based composites by incorporating graphene sheets into polymer matrices (*e.g.*, polystyrene).[53] This is a method for synthesizing graphene-based macroscopic structures at large scales. Unfortunately, as-obtained composites exhibit poor electrical conductivity (~0.1 S/m at 1 vol %).[53] One reason could be due to the high interfacial resistance established between graphene and the polymer matrix. In order to avoid this issue, an alternative strategy consists of directly assembling graphene sheets into 3D interconnected networks in the absence of any polymer matrix. Typical photographs and scanning electron microscopy (SEM) images can be found in Figure 5e−i. The electrical conductivity can be remarkably improved when compared to graphene−polymer matrices, even after incorporating these assemblies into a polymer matrix (*e.g.*, ~10 S/m at 0.5 wt % in poly(dimethylsiloxane)).[54] Besides having improved electrical conductivity, there are many other advantages derived from these 3D

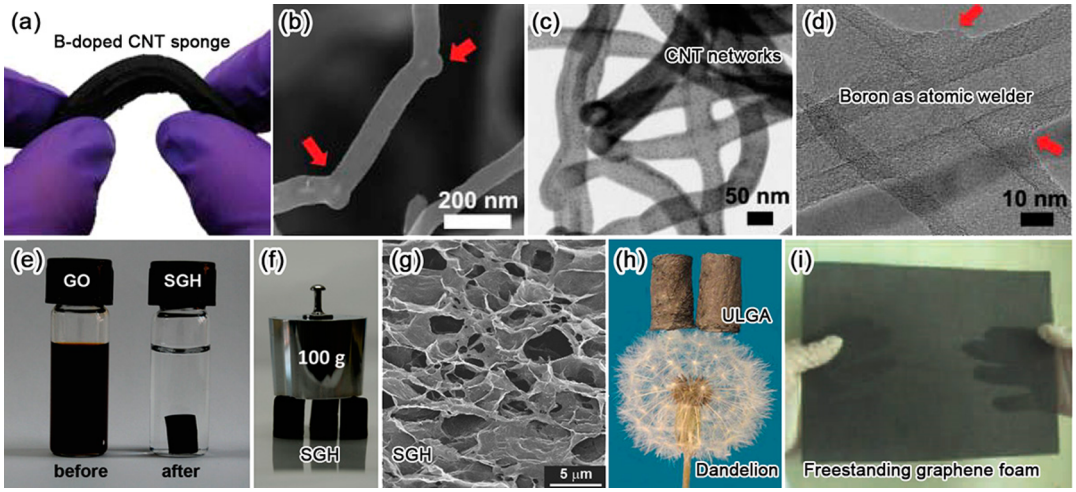

Figure 5. Three-dimensional covalent carbon nanotube networks and 3D graphene networks. (a) Photograph of 3D macroscopic B-doped CNT sponge. (b) Scanning electron microscopy image of the "elbow" defects found in B-doped CNT sponge. (c-d) Transmission electron microscopy images of the interconnected covalent nanojunctions in B-doped CNT sponge. Here, boron acts as an atomic welder. Adapted with permission from ref 43. Copyright 2012 Nature Publishing Group. (e) Photographs of a 2 mg/mL homogeneous GO aqueous dispersion before and after hydrothermal reduction at 180 °C for 12 h. (f) Photographs of a strong self-assembled graphene hydrogel (SGH). (g) SEM image of the SGH interior microstructures. Adapted from ref 64. Copyright 2010 American Chemical Society. (h) Photograph of two ultralight graphene aerogel (ULGA) samples rested on a dandelion. Adapted with permission from ref 58. Copyright 2013 Wiley-VCH Verlag GmbH & Co. KGaA, Weinheim. (i) Photograph of a 170 × 220 mm^2 free-standing graphene foam (GF) synthesized by using nickel foam as templates *via* CVD. Adapted with permission from ref 54. Copyright 2011 Nature Publishing Group.

graphene networks, such as high porosity,[55] good flexibility,[56] high elasticity,[57] ultralight weight,[58] high surface area,[55] superhydrophobicity,[59] *etc*. So far, much progress has been achieved along this line, although the final 3D graphene products were termed using different names, such as graphene hydrogels,[60] graphene foams,[54] graphene sponges,[61] graphene aerogels,[58] graphene monoliths,[57,62] strutted graphene,[63] *etc*. Regarding the synthesis methods for 3D graphene networks, they can be classified into two groups based on the way they are fabricated: rGO-based assembly methods and template-directed CVD growth. Due to the unique advantages in large-scale production of this top-down route, currently, rGO-based assembly methods appear to be widely used for producing 3D graphene networks. Self-assembly and reduction of GO into interconnected graphene networks are usually achieved by heat treating aqueous GO suspensions for a certain amount of time (*e.g.*, 1−12 h) inside containers (*e.g.*, 180 °C in a Teflon-lined autoclave,[55,64] 95−100 °C in a glass vial without stirring[58,65]). Subsequent freeze-drying is sometimes adopted to avoid serious volume shrinkage during the process of water removal in order to preserve the shape and porous 3D graphene-like structure.[66,67] It should be emphasized that the morphology and properties of the final products strongly depend on the concentration of GO (C_{GO}) in the aqueous suspensions. If C_{GO} is low (*e.g.*, 0.5 mg/mL), it has been demonstrated that only a black powdery material is produced after 12 h hydrothermal reduction.[64] In order to synthesize self-standing porous 3D graphene materials, a fairly high C_{GO} value (*e.g.*, 1.0−2.0 mg/mL) is necessary.[64] When compared to the rGO-based assembly methods, the template-directed CVD growth can produce seamless covalently interconnected 3D graphene networks with enhanced electronic conductivity inherited from the high-crystalline CVD-derived graphene sheets.[54] Usually, transition metal (*e.g.*, Ni, Cu) foams and hydrocarbons (*e.g.*, CH_4) are used as template materials and carbon sources for graphene growth, respectively.[54] After the metal foams are etched away, interconnected 3D graphene networks are finally obtained. It has been demonstrated that CVD-derived graphene networks can be used as a highly sensitive material for detecting toxic gases (*e.g.*, NO_2) in the parts per million range because the charge carrier transport through the 3D graphene networks is very sensitive to the adsorption/desorption of gaseous species.[68] Based on their excellent properties, 3D graphene networks could be used in many other fields, including flexible conductors,[54] supercapacitors,[64] solar cells,[69] microbial fuel cells,[70] Li−S batteries,[71] capture of cancer cells,[72] oil spill cleanup,[73] *etc*. More fascinating properties and applications will no doubt be developed in the future based on these unique 3D graphene networks, but various challenges will need to be overcome. Moreover, to the best of our knowledge, the atomic-scale identification of the 3D graphene network structure has not yet been carried out. It is also important to emphasize that, in 1991 and 1992, Mackay and Terrones[74] and Lenosky et al.,[75] respectively, proposed a negatively curved graphitic carbon structure, termed *Schwarzite* (see Figure 1i),

which was named in honor of the famous mathematician H. A. Schwarz, who first explored the triply periodic minimal surfaces. On the basis of the microscopic morphology of graphene networks, we envision that the negative curvature (*e.g.*, defects like the *heptagons*) is indeed crucial for the formation of the interconnected 3D graphene and other hybrid sp^2-hybridized carbon structures discussed here. The challenge remains: how to synthesize controllably and to identify such fascinating hypothetical hybrid systems.

Conflict of Interest: The authors declare no competing financial interest.

Acknowledgment. R.T.L. acknowledges financial support from the National Natural Science Foundation of China (Grant No. 51372131). The authors also acknowledge the U.S. Air Force Office of Scientific Research MURI Grant FA9550-12-1-0035.

REFERENCES AND NOTES

1. Kroto, H. W.; Heath, J. R.; Obrien, S. C.; Curl, R. F.; Smalley, R. E. C_{60}: Buckminsterfullerene. *Nature* **1985**, *318*, 162–163.
2. Oberlin, A.; Endo, M.; Koyama, T. Filamentous Growth of Carbon through Benzene Decomposition. *J. Cryst. Growth* **1976**, *32*, 335–349.
3. Iijima, S. Helical Microtubules of Graphitic Carbon. *Nature* **1991**, *354*, 56–58.
4. Li, X. L.; Wang, X. R.; Zhang, L.; Lee, S. W.; Dai, H. J. Chemically Derived, Ultrasmooth Graphene Nanoribbon Semiconductors. *Science* **2008**, *319*, 1229–1232.
5. Novoselov, K. S.; Geim, A. K.; Morozov, S. V.; Jiang, D.; Zhang, Y.; Dubonos, S. V.; Grigorieva, I. V.; Firsov, A. A. Electric Field Effect in Atomically Thin Carbon Films. *Science* **2004**, *306*, 666–669.
6. Yan, Z.; Peng, Z.; Casillas, G.; Lin, J.; Xiang, C.; Zhou, H.; Yang, Y.; Ruan, G.; Raji, A.-R. O.; Samuel, E. L. G.; *et al.* Rebar Graphene. *ACS Nano* **2014**, 10.1021/nn501132n.
7. Geim, A. K.; Novoselov, K. S. The Rise of Graphene. *Nat. Mater.* **2007**, *6*, 183–191.
8. Balandin, A. A.; Ghosh, S.; Bao, W. Z.; Calizo, I.; Teweldebrhan, D.; Miao, F.; Lau, C. N. Superior Thermal Conductivity of Single-Layer Graphene. *Nano Lett.* **2008**, *8*, 902–907.
9. Novoselov, K. S.; Jiang, Z.; Zhang, Y.; Morozov, S. V.; Stormer, H. L.; Zeitler, U.; Maan, J. C.; Boebinger, G. S.; Kim, P.; Geim, A. K. Room-Temperature Quantum Hall Effect in Graphene. *Science* **2007**, *315*, 1379.
10. Stankovich, S.; Dikin, D. A.; Piner, R. D.; Kohlhaas, K. A.; Kleinhammes, A.; Jia, Y.; Wu, Y.; Nguyen, S. T.; Ruoff, R. S. Synthesis of Graphene-Based Nanosheets *via* Chemical Reduction of Exfoliated Graphite Oxide. *Carbon* **2007**, *45*, 1558–1565.
11. Kim, K. S.; Zhao, Y.; Jang, H.; Lee, S. Y.; Kim, J. M.; Kim, K. S.; Ahn, J. H.; Kim, P.; Choi, J. Y.; Hong, B. H. Large-Scale Pattern Growth of Graphene Films for Stretchable Transparent Electrodes. *Nature* **2009**, *457*, 706–710.
12. Li, X. S.; Cai, W. W.; An, J. H.; Kim, S.; Nah, J.; Yang, D. X.; Piner, R.; Velamakanni, A.; Jung, I.; Tutuc, E.; *et al.* Large-Area Synthesis of High-Quality and Uniform Graphene Films on Copper Foils. *Science* **2009**, *324*, 1312–1314.
13. Cai, J. M.; Ruffieux, P.; Jaafar, R.; Bieri, M.; Braun, T.; Blankenburg, S.; Muoth, M.; Seitsonen, A. P.; Saleh, M.; Feng, X. L.; *et al.* Atomically Precise Bottom-Up Fabrication of Graphene Nanoribbons. *Nature* **2010**, *466*, 470–473.
14. Park, S.; Ruoff, R. S. Chemical Methods for the Production of Graphenes. *Nat. Nanotechnol.* **2009**, *4*, 217–224.
15. Lee, C.; Wei, X. D.; Kysar, J. W.; Hone, J. Measurement of the Elastic Properties and Intrinsic Strength of Monolayer Graphene. *Science* **2008**, *321*, 385–388.
16. Novaes, F. D.; Rurali, R.; Ordejón, P. Electronic Transport between Graphene Layers Covalently Connected by Carbon Nanotubes. *ACS Nano* **2010**, *4*, 7596–7602.
17. Varshney, V.; Patnaik, S. S.; Roy, A. K.; Froudakis, G.; Farmer, B. L. Modeling of Thermal Transport in Pillared-Graphene Architectures. *ACS Nano* **2010**, *4*, 1153–1161.
18. Dimitrakakis, G. K.; Tylianakis, E.; Froudakis, G. E. Pillared Graphene: A New 3-D Network Nanostructure for Enhanced Hydrogen Storage. *Nano Lett.* **2008**, *8*, 3166–3170.
19. Lin, X. Y.; Liu, P.; Wei, Y.; Li, Q. Q.; Wang, J. P.; Wu, Y.; Feng, C.; Zhang, L. N.; Fan, S. S.; Jiang, K. L. Development of an Ultra-thin Film Composed of a Graphene Membrane and Carbon Nanotube Vein Support. *Nat. Commun.* **2013**, *4*, 2920.
20. Li, Y. G.; Zhou, W.; Wang, H. L.; Xie, L. M.; Liang, Y. Y.; Wei, F.; Idrobo, J. C.; Pennycook, S. J.; Dai, H. J. An Oxygen Reduction Electrocatalyst Based on Carbon Nanotube-Graphene Complexes. *Nat. Nanotechnol.* **2012**, *7*, 394–400.
21. Lv, R. T.; Cui, T. X.; Jun, M. S.; Zhang, Q.; Cao, A. Y.; Su, D. S.; Zhang, Z. J.; Yoon, S. H.; Miyawaki, J.; Mochida, I.; *et al.* Open-Ended, N-Doped Carbon Nanotube–Graphene Hybrid Nanostructures as High-Performance Catalyst Support. *Adv. Funct. Mater.* **2011**, *21*, 999–1006.
22. Hong, T. K.; Lee, D. W.; Choi, H. J.; Shin, H. S.; Kim, B. S. Transparent, Flexible Conducting Hybrid Multilayer Thin Films of Multiwalled Carbon Nanotubes with Graphene Nanosheets. *ACS Nano* **2010**, *4*, 3861–3868.
23. Fan, Z. J.; Yan, J.; Zhi, L. J.; Zhang, Q.; Wei, T.; Feng, J.; Zhang, M. L.; Qian, W. Z.; Wei, F. A Three-Dimensional Carbon Nanotube/Graphene Sandwich and Its Application as Electrode in Supercapacitors. *Adv. Mater.* **2010**, *22*, 3723–3728.
24. Zhu, Y.; Li, L.; Zhang, C. G.; Casillas, G.; Sun, Z. Z.; Yan, Z.; Ruan, G. D.; Peng, Z. W.; Raji, A. R. O.; Kittrell, C.; *et al.* A Seamless Three-Dimensional Carbon Nanotube Graphene Hybrid Material. *Nat. Commun.* **2012**, *3*, 1225.
25. Tristan-Lopez, F.; Morelos-Gomez, A.; Vega-Diaz, S. M.; Garcia-Betancourt, M. L.; Perea-Lopez, N.; Elias, A. L.; Muramatsu, H.; Cruz-Silva, R.; Tsuruoka, S.; Kim, Y. A.; *et al.* Large Area Films of Alternating Graphene-Carbon Nanotube Layers Processed in Water. *ACS Nano* **2013**, *7*, 10788–10798.
26. Lee, D. H.; Kim, J. E.; Han, T. H.; Hwang, J. W.; Jeon, S.; Choi, S. Y.; Hong, S. H.; Lee, W. J.; Ruoff, R. S.; Kim, S. O. Versatile Carbon Hybrid Films Composed of Vertical Carbon Nanotubes Grown on Mechanically Compliant Graphene Films. *Adv. Mater.* **2010**, *22*, 1247–1252.
27. Jiang, K. L.; Li, Q. Q.; Fan, S. S. Nanotechnology: Spinning Continuous Carbon Nanotube Yarns. *Nature* **2002**, *419*, 801.
28. Zhang, M.; Fang, S. L.; Zakhidov, A. A.; Lee, S. B.; Aliev, A. E.; Williams, C. D.; Atkinson, K. R.; Baughman, R. H. Strong, Transparent, Multifunctional, Carbon Nanotube Sheets. *Science* **2005**, *309*, 1215–1219.
29. Feng, C.; Liu, K.; Wu, J. S.; Liu, L.; Cheng, J. S.; Zhang, Y. Y.; Sun, Y. H.; Li, Q. Q.; Fan, S. S.; Jiang, K. L. Flexible, Stretchable, Transparent Conducting Films Made from Superaligned Carbon Nanotubes. *Adv. Funct. Mater.* **2010**, *20*, 885–891.
30. Zhang, Q.; Wang, D. G.; Huang, J. Q.; Zhou, W. P.; Luo, G. H.; Qian, W. Z.; Wei, F. Dry Spinning Yarns from Vertically Aligned Carbon Nanotube Arrays Produced by an Improved Floating Catalyst Chemical Vapor Deposition Method. *Carbon* **2010**, *48*, 2855–2861.
31. Beliatis, M. J.; Gandhi, K. K.; Rozanski, L. J.; Rhodes, R.; McCafferty, L.; Alenezi, M. R.; Alshammari, A. S.; Mills, C. A.; Jayawardena, K. D. G. I.; Henley, S. J.; *et al.* Hybrid Graphene–Metal Oxide Solution Processed Electron Transport Layers for Large Area High-Performance Organic Photovoltaics. *Adv. Mater.* **2014**, *26*, 2078–2083.
32. Cohen-Tanugi, D.; Grossman, J. C. Water Desalination across Nanoporous Graphene. *Nano Lett.* **2012**, *12*, 3602–3608.
33. Elias, A. L.; Perea-Lopez, N.; Rajukumar, L. P.; McCreary, A.; Lopez-Urias, F.; Terrones, H.; Terrones, M. Three-Dimensional Nanotube Networks and a New Horizon of Applications. In *Nanotube Superfiber Materials*;

Schulz, M. J., Shanov, V. N., Yin, Z., Eds.; Elsevier Inc.: Amsterdam, 2014; pp 457−493.
34. Iijima, S.; Ichihashi, T. Single-Shell Carbon Nanotubes of 1-nm Diameter. *Nature* **1993**, *363*, 603–605.
35. Bethune, D. S.; Kiang, C. H.; Devries, M. S.; Gorman, G.; Savoy, R.; Vazquez, J.; Beyers, R. Cobalt-Catalyzed Growth of Carbon Nanotubes with Single-Atomic-Layer Walls. *Nature* **1993**, *363*, 605–607.
36. Lambin, P.; Fonseca, A.; Vigneron, J. P.; Nagy, J. B.; Lucas, A. A. Structural and Electronic-Properties of Bent Carbon Nanotubes. *Chem. Phys. Lett.* **1995**, *245*, 85–89.
37. Romo-Herrera, J. M.; Terrones, M.; Terrones, H.; Dag, S.; Meunier, V. Covalent 2D and 3D Networks from 1D Nanostructures: Designing New Materials. *Nano Lett.* **2007**, *7*, 570–576.
38. Li, J.; Papadopoulos, C.; Xu, J. Nanoelectronics: Growing Y-Junction Carbon Nanotubes. *Nature* **1999**, *402*, 253–254.
39. Meng, G. W.; Jung, Y. J.; Cao, A. Y.; Vajtai, R.; Ajayan, P. M. Controlled Fabrication of Hierarchically Branched Nanopores, Nanotubes, and Nanowires. *Proc. Natl. Acad. Sci. U.S.A.* **2005**, *102*, 7074–7078.
40. Fu, Y.; Carlberg, B.; Lindahl, N.; Lindvall, N.; Bielecki, J.; Matic, A.; Song, Y.; Hu, Z.; Lai, Z.; Ye, L.; *et al.* Templated Growth of Covalently Bonded Three-Dimensional Carbon Nanotube Networks Originated from Graphene. *Adv. Mater.* **2012**, *24*, 1576–1581.
41. Terrones, M.; Banhart, F.; Grobert, N.; Charlier, J. C.; Terrones, H.; Ajayan, P. M. Molecular Junctions by Joining Single-Walled Carbon Nanotubes. *Phys. Rev. Lett.* **2002**, *89*, 075505.
42. Rodriguez-Manzo, J. A.; Wang, M. S.; Banhart, F.; Bando, Y.; Golberg, D. Multibranched Junctions of Carbon Nanotubes *via* Cobalt Particles. *Adv. Mater.* **2009**, *21*, 4477–4482.
43. Hashim, D. P.; Narayanan, N. T.; Romo-Herrera, J. M.; Cullen, D. A.; Hahm, M. G.; Lezzi, P.; Suttle, J. R.; Kelkhoff, D.; Munoz-Sandoval, E.; Ganguli, S.; *et al.* Covalently Bonded Three-Dimensional Carbon Nanotube Solids *via* Boron Induced Nanojunctions. *Sci. Rep.* **2012**, *2*, 363.
44. Romo-Herrera, J. M.; Sumpter, B. G.; Cullen, D. A.; Terrones, H.; Cruz-Silva, E.; Smith, D. J.; Meunier, V.; Terrones, M. An Atomistic Branching Mechanism for Carbon Nanotubes: Sulfur as the Triggering Agent. *Angew. Chem., Int. Ed.* **2008**, *47*, 2948–2953.
45. Lepro, X.; Vega-Cantu, Y.; Rodriguez-Macias, F. J.; Bando, Y.; Golberg, D.; Terrones, M. Production and Characterization of Coaxial Nanotube Junctions and Networks of CNx/CNT. *Nano Lett.* **2007**, *7*, 2220–2226.
46. Yu, H.; Li, Z. F.; Luo, G. H.; Wei, F. Growth of Branch Carbon Nanotubes on Carbon Nanotubes as Support. *Diamond Relat. Mater.* **2006**, *15*, 1447–1451.
47. Jo, J. W.; Jung, J. W.; Lee, J. U.; Jo, W. H. Fabrication of Highly Conductive and Transparent Thin Films from Single-Walled Carbon Nanotubes Using a New Non-ionic Surfactant *via* Spin Coating. *ACS Nano* **2010**, *4*, 5382–5388.
48. Gracia-Espino, E.; Sala, G.; Pino, F.; Halonen, N.; Luomahaara, J.; Maklin, J.; Toth, G.; Kordas, K.; Jantunen, H.; Terrones, M.; *et al.* Electrical Transport and Field-Effect Transistors Using Inkjet-Printed SWCNT Films Having Different Functional Side Groups. *ACS Nano* **2010**, *4*, 3318–3324.
49. Gui, E. L.; Li, L. J.; Zhang, K. K.; Xu, Y. P.; Dong, X. C.; Ho, X. N.; Lee, P. S.; Kasim, J.; Shen, Z. X.; Rogers, J. A.; *et al.* DNA Sensing by Field-Effect Transistors Based on Networks of Carbon Nanotubes. *J. Am. Chem. Soc.* **2007**, *129*, 14427–14432.
50. Aliev, A. E.; Oh, J. Y.; Kozlov, M. E.; Kuznetsov, A. A.; Fang, S. L.; Fonseca, A. F.; Ovalle, R.; Lima, M. D.; Haque, M. H.; Gartstein, Y. N.; *et al.* Giant-Stroke, Superelastic Carbon Nanotube Aerogel Muscles. *Science* **2009**, *323*, 1575–1578.
51. Chakrapani, N.; Wei, B. Q.; Carrillo, A.; Ajayan, P. M.; Kane, R. S. Capillarity-Driven Assembly of Two-Dimensional Cellular Carbon Nanotube Foams. *Proc. Natl. Acad. Sci. U.S.A.* **2004**, *101*, 4009–4012.
52. Cohen, D. J.; Mitra, D.; Peterson, K.; Maharbiz, M. M. A Highly Elastic, Capacitive Strain Gauge Based on Percolating Nanotube Networks. *Nano Lett.* **2012**, *12*, 1821–1825.
53. Stankovich, S.; Dikin, D. A.; Dommett, G. H. B.; Kohlhaas, K. M.; Zimney, E. J.; Stach, E. A.; Piner, R. D.; Nguyen, S. T.; Ruoff, R. S. Graphene-Based Composite Materials. *Nature* **2006**, *442*, 282–286.
54. Chen, Z. P.; Ren, W. C.; Gao, L. B.; Liu, B. L.; Pei, S. F.; Cheng, H. M. Three-Dimensional Flexible and Conductive Interconnected Graphene Networks Grown by Chemical Vapour Deposition. *Nat. Mater.* **2011**, *10*, 424–428.
55. Zhang, L.; Zhang, F.; Yang, X.; Long, G. K.; Wu, Y. P.; Zhang, T. F.; Leng, K.; Huang, Y.; Ma, Y. F.; Yu, A.; *et al.* Porous 3D Graphene-Based Bulk Materials with Exceptional High Surface Area and Excellent Conductivity for Supercapacitors. *Sci. Rep.* **2013**, *3*, 1408.
56. Xu, Y.; Lin, Z.; Huang, X.; Liu, Y.; Huang, Y.; Duan, X. Flexible Solid-State Supercapacitors Based on Three-Dimensional Graphene Hydrogel Films. *ACS Nano* **2013**, *7*, 4042–4049.
57. Qiu, L.; Liu, J. Z.; Chang, S. L. Y.; Wu, Y. Z.; Li, D. Biomimetic Superelastic Graphene-Based Cellular Monoliths. *Nat. Commun.* **2012**, *3*, 1241.
58. Hu, H.; Zhao, Z. B.; Wan, W. B.; Gogotsi, Y.; Qiu, J. S. Ultralight and Highly Compressible Graphene Aerogels. *Adv. Mater.* **2013**, *25*, 2219–2223.
59. Singh, E.; Chen, Z. P.; Houshmand, F.; Ren, W. C.; Peles, Y.; Cheng, H. M.; Koratkar, N. Superhydrophobic Graphene Foams. *Small* **2013**, *9*, 75–80.
60. Xu, Y.; Wu, Q.; Sun, Y.; Bai, H.; Shi, G. Three-Dimensional Self-Assembly of Graphene Oxide and DNA into Multifunctional Hydrogels. *ACS Nano* **2010**, *4*, 7358–7362.
61. Liu, F.; Seo, T. S. A Controllable Self-Assembly Method for Large-Scale Synthesis of Graphene Sponges and Free-Standing Graphene Films. *Adv. Funct. Mater.* **2010**, *20*, 1930–1936.
62. Tao, Y.; Kong, D. B.; Zhang, C.; Lv, W.; Wang, M. X.; Li, B. H.; Huang, Z. H.; Kang, F. Y.; Yang, Q. H. Monolithic Carbons with Spheroidal and Hierarchical Pores Produced by the Linkage of Functionalized Graphene Sheets. *Carbon* **2014**, *69*, 169–177.
63. Wang, X. B.; Zhang, Y. J.; Zhi, C. Y.; Wang, X.; Tang, D. M.; Xu, Y. B.; Weng, Q. H.; Jiang, X. F.; Mitome, M.; Golberg, D.; *et al.* Three-Dimensional Strutted Graphene Grown by Substrate-Free Sugar Blowing for High-Power-Density Supercapacitors. *Nat. Commun.* **2013**, *4*, 2905.
64. Xu, Y. X.; Sheng, K. X.; Li, C.; Shi, G. Q. Self-Assembled Graphene Hydrogel *via* a One-Step Hydrothermal Process. *ACS Nano* **2010**, *4*, 4324–4330.
65. Xu, Y.; Lin, Z.; Huang, X.; Wang, Y.; Huang, Y.; Duan, X. Functionalized Graphene Hydrogel-Based High-Performance Supercapacitors. *Adv. Mater.* **2013**, *25*, 5779–5784.
66. Wu, Z.-S.; Winter, A.; Chen, L.; Sun, Y.; Turchanin, A.; Feng, X.; Müllen, K. Three-Dimensional Nitrogen and Boron Co-doped Graphene for High-Performance All-Solid-State Supercapacitors. *Adv. Mater.* **2012**, *24*, 5130–5135.
67. Tao, Y.; Xie, X. Y.; Lv, W.; Tang, D. M.; Kong, D. B.; Huang, Z. H.; Nishihara, H.; Ishii, T.; Li, B. H.; Golberg, D.; Kang, F. Y.; *et al.* Towards Ultrahigh Volumetric Capacitance: Graphene Derived Highly Dense but Porous Carbons for Supercapacitors. *Sci. Rep.* **2013**, *3*, 2975.
68. Yavari, F.; Chen, Z. P.; Thomas, A. V.; Ren, W. C.; Cheng, H. M.; Koratkar, N. High Sensitivity Gas Detection Using a Macroscopic Three-Dimensional Graphene Foam Network. *Sci. Rep.* **2011**, *1*, 166.
69. Xue, Y. H.; Liu, J.; Chen, H.; Wang, R. G.; Li, D. Q.; Qu, J.; Dai, L. M. Nitrogen-Doped Graphene Foams as Metal-Free Counter Electrodes in High-Performance Dye-Sensitized Solar Cells. *Angew. Chem., Int. Ed.* **2012**, *51*, 12124–12127.
70. Xie, X.; Yu, G. H.; Liu, N.; Bao, Z. N.; Criddle, C. S.; Cui, Y. Graphene-Sponges as High-Performance Low-Cost Anodes for Microbial Fuel Cells. *Energy Environ. Sci.* **2012**, *5*, 6862–6866.
71. Zhao, M.-Q.; Zhang, Q.; Huang, J.-Q.; Tian, G.-L.; Nie, J.-Q.; Peng, H.-J.; Wei, F. Unstacked Double-Layer Templated Graphene for High-Rate

Lithium–Sulphur Batteries. *Nat. Commun.* **2014**, *5*, 3410.
72. Yin, S.; Wu, Y.-L.; Hu, B.; Wang, Y.; Cai, P.; Tan, C. K.; Qi, D.; Zheng, L.; Leow, W. R.; Tan, N. S.; *et al.* Three-Dimensional Graphene Composite Macroscopic Structures for Capture of Cancer Cells. *Adv. Mater. Interfaces* **2014**, 10.1002/admi.201300043.
73. Li, H.; Liu, L. F.; Yang, F. L. Covalent Assembly of 3D Graphene/Polypyrrole Foams for Oil Spill Cleanup. *J. Mater. Chem. A* **2013**, *1*, 3446–3453.
74. Mackay, A. L.; Terrones, H. Diamond from Graphite. *Nature* **1991**, *352*, 762–762.
75. Lenosky, T.; Gonze, X.; Teter, M.; Elser, V. Energetics of Negatively Curved Graphitic Carbon. *Nature* **1992**, *355*, 333–335.